14

Gold and Silver Nanowires for Fluorescence Enhancement

Krystyna Drozdowicz-Tomsia and Ewa M. Goldys
MQ BioFocus Research Centre, Macquarie University, NSW, Australia

1. Introduction

One-dimensional (1-D) noble metallic nanoscale materials, particularly silver or gold have been attracting wide interest due to their unique optical, electronic, catalytic and mechanical properties. Recently significant interest has been devoted to ultrasensitive detection of trace analytes down to a single molecule level. Various strategies to lower the detection limit for fluorescence-based sensors include increasing the signal from fluorescent dyes that indicate the presence of a specific analyte. Metals such as gold and silver with nanometer scale dimensions (in the 1-100 nm range) exhibit a remarkable optical effect known as localised surface plasmon resonance (Hutter and Fendler 2001, Lakowicz et all 2002 and 2003, Geddes et all 2003a, Geddes et all 2003b,Liebermann and Knoll 2000, Tarcha et all 1998, Tarcha et all 1999, Sokolov et all 1998, Kummerlen et all 1993, Felidi et all 1999, Jensen at all 2000), which is due to resonant photons inducing coherent surface plasmon oscillations of their conduction band electrons. The confinement of the surface plasmon resonance to the nanoparticle dimensions can increase the amplitude of electromagnetic wave by as much as orders of magnitude. This strong electromagnetic field decays exponentially over a distance comparable with nanostructures size. Correspondingly, light intensity near such nanostructures (proportional to the square of the wave's amplitude) is also significantly increased. In such a way noble metal particles through plasmonic confinement, effectively focus resonantly coupled light. As a result, all radiative properties of molecules in proximity of such nanoparticles, such as light absorption, fluorescence, Rayleigh scattering and Raman scattering can be enhanced by orders of magnitude, when certain conditions are met. In particular, metal nanoparticles can modify the properties of close fluorophores. The presence of a nearby metallic nanoparticle can not only enhance fluorophore quantum yield but also stabilize adjacent fluorophores against photobleaching, further enhancing their utility in fluorescence sensing and imaging. However, when fluorophores are very close to the metal surface, the fluorescence quenching effect competes with these favorable effects[2] and it dominates within 5 nm from the surface of metallic particles. At larger distances, the enhancement starts to override the quenching and it reaches its maximum at about 10 nm from the metal surface (Kerker et all 1982, Gersten and Nitzan 1985). At larger metal-fluorophore separation, the enhancement effect progressively decreases. Early studies using colloidal silver or silver fractals deposited electrochemically on glass substrates showed substantial enhancement of fluorescence in the visible range (Geddes et at all 2003a, 2003b, Sokolov et all 1998, Kummerlen et all 1993). Larger enhancements were created using more

precisely controlled, regular arrangements of noble metal nano-structures (Corrigan at all 2006, Corrigan et all 2005). Uniform arrays of nanostructures produced narrower resonances; allowing better control of the scattered light and optimization of spectral overlap between the metal particle plasmon resonances and absorption/emission of fluorescent molecules. Fluorescence intensities of up to 350 times of the original value on a bare glass surface had been observed for Ag nanoparticles on an "active" substrate (Guo et all 2008a, Guo at all 2008b) and even higher enhancement factors have been theoretically predicted.

Since last decade it has been anticipated that noble metal nanorods and nanowires offer exceptional potential to modify electromagnetic fields, on the basis of their apparent similarities to simple antennas. Indeed, Schatz et al (Hao and Schatz 2004) have theoretically calculated that isolated nanorods and nanowires show the highest electromagnetic (EM) field enhancement at their ends compared to other nanoparticle shapes, making them potentially attractive substrates for metal enhanced fluorescence (MEF), but very few reports to-date have reported relevant experiments. In our previous work (Goldys at all 2007) we showed that the nanowires were responsible for the fluorescence amplification factors of up to two orders of magnitude. Such amplification factors were induced by plasmon resonance in the nanowires but they were also due to the fact that these nanowires with high aspect ratio and sharp tips act as antennas for the radiating emission from fluorophores. Even higher enhancements can be expected for nanorods aligned end-to-end in one dimension. In such configuration large electromagnetic fields at the neighbouring nanorods can be coupled and used for sensing of single molecules.

In this chapter we explain unique, highly tuneable optical properties of gold and silver nanorods and briefly describe their synthesis. Further, we discuss functionalisation of silver and gold nanorods, designed to bind these nanorods to proteins labelled with fluorophores. These fluorophores are selected so that their excitation-emission characteristics provide the best overlap with plasmon resonances. These nanorods are then used to form well controlled arrays on glass substrates. Here we discuss various arrangements including glass substrates with thin continuous noble metal layer separated by a dielectric spacer from the nanorods. We also show various nanoantenna designs, modelled using Finite Element Method, which are able to efficiently couple light in and out of fluorophores.

2. Optical properties of metal nanorods and their effect on fluorescence enhancement

The extinction spectrum of metal nanoparticles consists of two components: scattering and absorption, whose relative contributions depends on size and shape of the nanoparticle. The scattering component is known to be responsible for fluorescence enhancement and the absorption component for fluorescence quenching. Another important parameter, the scattering quantum yield, η, was defined by El Sayed *et al*. (Lee and El-Sayed 2005) as the ratio of the scattering cross section σ_{sca} to the extinction cross section σ_{ext} of the nanoparticle:

$$\sigma_{ext} = \sigma_{abs} + \sigma_{sca} \tag{1}$$

$$\eta = \sigma_{sca} / \sigma_{ext} \tag{2}$$

Here the extinction cross section is obtained from the imaginary part of the nanoparticle polarizability α and k is the wavevector of light ($k=2\pi/\lambda$):

$$\sigma_{ext} = k\,\mathrm{Im}(\alpha) \tag{3}$$

The scattering cross-section is also related to polarisability as:

$$\sigma_{sca} = \frac{k^4}{6\pi}|\alpha|^2 \tag{4}$$

The polarizability is defined through the relationship of the dipole moment p induced by the applied field E_0

$$p = \alpha E_0 \tag{5}$$

In order for metal nanoparticles to strongly enhance fluorescence several conditions must be met. One of the most important is the spectral overlap of the resonant plasmon position in the metal nanoparticle with excitation/emission spectrum of the fluorophore (Chen et all 2007). The fluorescence enhancement also depends on nanoparticle geometry. This is because only the scattering component of the extinction spectrum of metal nanoparticles contributes to the fluorescence enhancement and its magnitude compared to the absorption component depends on size. For example, it starts to dominate for spherical nanoparticles larger than ~50 nm for silver and ~80 nm for gold. Another important aspect of the plasmon resonance is its linewidth as narrow resonances lead to higher enhancements and higher sensitivity to the local changes in dielectric constant of the environment, which can be also used for molecular sensing. When plasmon oscillations are generated in the metal nanoparticle, they are subject to a number of processes which dampen the collective oscillations and result in the plasmons decay. The plasmon resonance linewidth is inversely proportional to the lifetime of the plasmon and it provides a measure of this decay process. Damping can occur either through radiative or nonradiative processes. Radiative damping occurs when the oscillating dipole moment of the plasmon gives rise to photon emission. Nonradiative damping occurs when the plasmon excites intraband or interband electronic transitions within metal particle or through electron scattering processes at the surface of the nanostructure. Plasmon position and near-field electric fields created near metal particles can be additionally very strongly affected by nanostructure arrangement.

Metal nanostructures can enhance or quench fluorescence by modifying radiative and non-radiative emission rates of the fluorophore as a result of interactions of their plasmon resonances with absorption/emission bands of fluorophore. This effect is observed by changes in fluorophore quantum yield, and its lifetime. Nanorods have particularly favourable optical properties for fluorescence enhancement due to their high tunability of position of plasmon resonances, polarization sensitivity and their long dephasing times leading to strong, narrow spectral resonances.

2.1 Tunability of resonance

In 1912, Gans (Gans 1915) predicted that for very small ellipsoids, where the dipole approximation is satisfied, the surface plasmon mode splits into two distinct modes. This is a consequence of the surface curvature, which classically determines the restoring force or depolarization field that acts on the population of confined conduction electrons. He quantified the response as a function of the ellipsoid aspect ratio. For such oblate and prolate spheroid geometry analytical solutions have been found. In this case methods such as discrete dipole approximation (DDA) and numerical calculations such as T-matrix

method are commonly used. Schatz and co-workers have recently reviewed this computational approach (Kelly at all 2003), which can be successfully applied to nanorods, nanowires and nanocylinder structures as confirmed by very good agreement of the calculated and experimentally measured resonance spectra for such particles.
According to Gans's formula, the polarizability of an ellipsoidal metal particle along the x (y,z) axis is given by:

$$\alpha_{x,y,z} = \frac{4}{3}\pi\, abc \frac{(\varepsilon_m - \varepsilon_0)}{\varepsilon_{m+L_{x,y,z}}(\varepsilon_m - \varepsilon_0)} \tag{6}$$

Here a, b and c refer to the length of the ellipse along the x, y and z axes ($a > b = c$), ε_m is the dielectric function of metal, ε_0 the dielectric constant of the medium at optical frequencies and $L_{x,y,z}$ is the depolarization factor for the respective axis, which is given by:

$$L_x = \frac{1-e^2}{e^2}\left(-1 + \frac{1}{2e} ln \frac{1+e}{1-e}\right); \tag{7}$$

$$L_{y,z} = \frac{1-L_x}{2} \tag{8}$$

Here, e is the rod ellipticity given by $e^2 = 1-(b/a)^2$ which can be also rearranged and expressed as a function of the aspect ratio $R = b/a$. For a sphere $e = 0$ and $L = 1/3$ and Equation /6/ becomes:

$$\alpha_0 = 3V \frac{\varepsilon_m - \varepsilon_0}{\varepsilon_m + 2\varepsilon_0} \tag{9}$$

where V is the nanoparticle volume. As it is clearly seen by comparing equations /6/ and /9/, for the same effective volume of the nanoparticle, the spectral tunability of the plasmon resonance for elliptical particle is much larger, and it is more sensitive to the aspect ratio than to the absolute particle size.
Finally the extinction of light is related directly to the polarizability by relationship in Equation /3/ and for an assembly of randomly oriented N ellipsoids the extinction coefficient γ can be calculated according to Gans formula.

$$\gamma = \frac{2\pi NV\varepsilon_0^{3/2}}{3\lambda} \sum_{x,y,z} \frac{(\frac{1}{L_{x,y,z}^2})\varepsilon_{m2}}{\left(\varepsilon_{m1} + \frac{1-L_{x,y,z}}{L_{x,y,z}}\right)^2 + \varepsilon_{m2}^2} \tag{10}$$

where V is particle volume and ε_{m1} and ε_{m2} are real and imaginary components of dielectric function of metal nanoparticle and λ is the incident light wavelength.
For ellipsoidal nanoparticles the resonances for light polarized in the longitudinal (LE) direction (along the long axis of the particle) and in transverse (TE) direction are different, hence two peaks are observed in the absorption spectra for randomly oriented assembly of nanorods corresponding to LE and TE modes as calculated according to Equation /10/ and shown in Figure 1.
These relationships show that size and shape of the nanoparticle can control the plasmonic resonances, and thus by varying nanoparticle geometry it is possible to synthesize materials with tuneable extinction spectra. Gans's equations also predict that the LSPR position varies linearly with aspect ratio for small ellipsoids embedded in the same medium and that for the same aspect ratio nanoparticles their plasmon peak position will red shift, when the dielectric function of the surrounding medium increases. These attractive properties

motivated intense experimental efforts to develop controlled synthesis of metal nanorods summarised recently in several reviews (Huang et all 2009, Perez-Juste et all 2005).

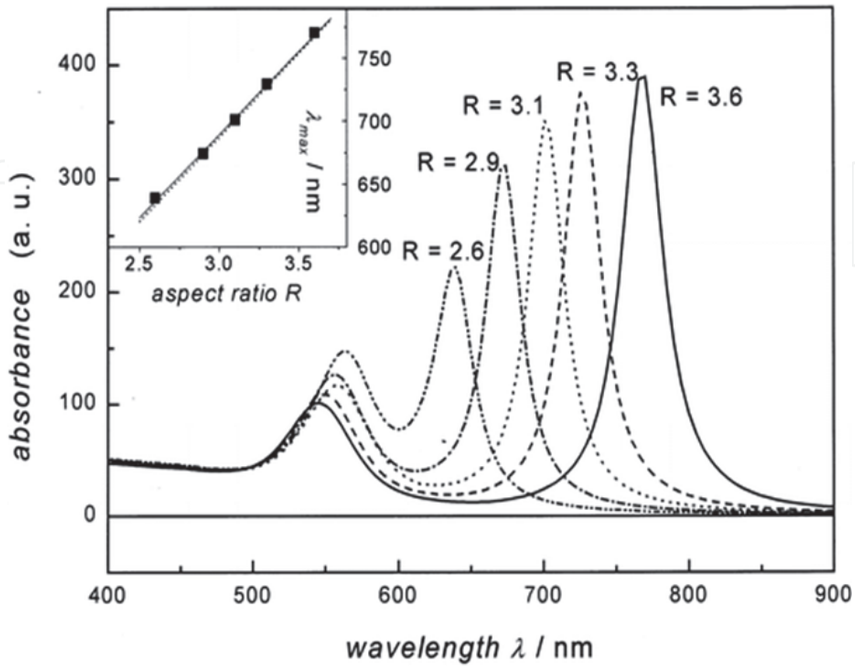

Fig. 1. Calculated absorption spectra of elongated ellipsoids with varying aspect ratios R using Equation /10/. The medium dielectric constant was fixed at a value of 4. The short wavelength peak corresponds to the transverse mode resonance, and the long wavelength one to longitudinal resonance which is very sensitive to the aspect ratio R. The inset shows a plot of the peak of the longitudinal plasmon band determined from the calculated spectra as a function of the aspect ratio. The solid line is a linear fit to the data points. (Reprinted from Reference Link at all 1999).

Figure 2 shows that by varying the aspect ratio of gold nanorods it is possible to adjust the plasmon resonance position in a broad spectral range (530 – 1200 nm), but the optimum scattering efficiency is reached for the nanorods with an aspect ratio of 3.4 (Figure 2 b) and for the rod diameter of 60 nm (Figure 2 c). The double peak character of extinction spectra for nanorods allows to predict that uniformly oriented ellipsoids and cylinders should exhibit strong, polarization-dependent optical spectra with tunability of enhancement for two different fluorophores.

Khlebtsov at all (Klebtsov 2007) used T-matrix formalism to study the multipole resonances in long gold and silver nanorods whose shape was modeled by prolate spheroids and cylinders with flat or semispherical ends. The particle diameters and aspect ratio were varied from 20 to 80 nm and from 2 to 20, respectively. They found that the parity of a given spectral resonance number n coincides with the parity of their multipole contributions l, where l is equal to or greater than n, and the total resonance magnitude is determined by the lowest multipole contribution. According to their calculations, multipole resonance wavelengths also obey a universal linear scaling behaviour when plotted versus the particle aspect ratio divided by the resonance number. This remarkable property of multipole resonances can be understood in terms of a simple concept based on plasmon standing waves excited in metal nanowires by an

electric field of incident light (Schider et all 2003). The refractive index sensitivity of the multipole resonance wavelength to a dielectric environment also exhibits linear scaling properties. Specifically, the relative shift of the resonance wavelength is proportional to the relative refractive index increment with a universal angular slope coefficient.

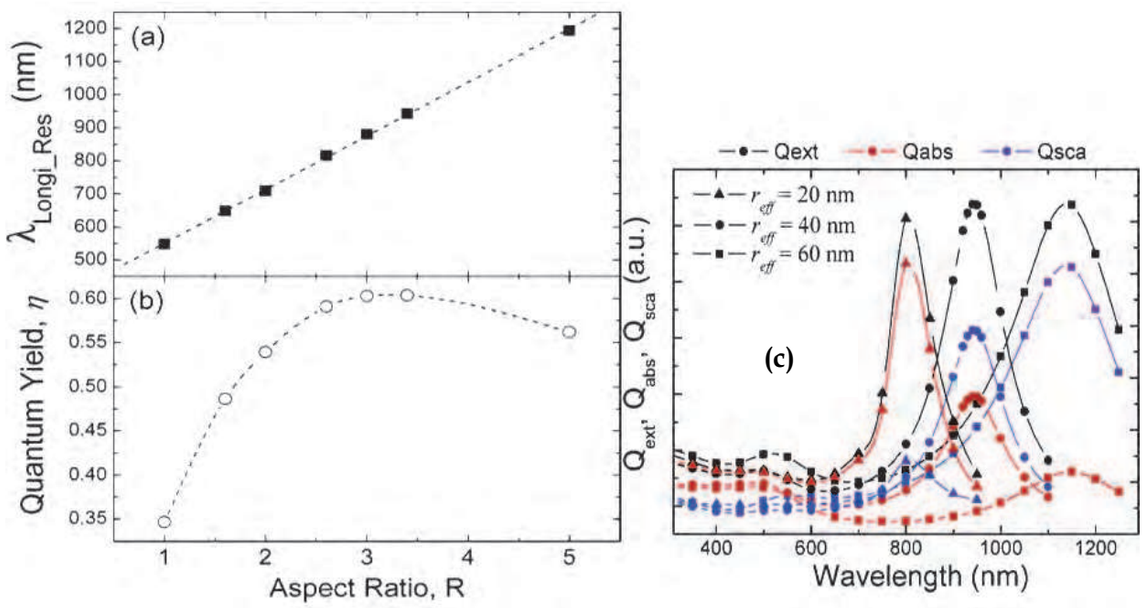

Fig. 2. (a) Dependence of the plasmon peak wavelength and (b) scattering quantum yield of the longitudinal surface plasmon resonance on the aspect ratio. Unlike resonance wavelength, which shows a linear relationship with the nanorod aspect ratio R, the scattering quantum yield increases with increasing R, reaching a maximum at 3.4, and begins to decrease from then on.(c) Relative contributions of light scattering and absorption to the total extinction efficiency for various rod diameters at a fixed aspect ratio of 3.4 for rods illuminated by light polarized in longitudinal direction. Reproduced from Ref. (Lee et all 2006).

2.2 Surface plasmon resonance linewidth and dephasing time

Sönnichsen (Sonnichen et all 2002) and co-workers studied the dephasing of plasmons in single gold nanoparticles and their results are presented in Figure 3. They have found a pronounced reduction of the plasmon dephasing rate in nanorods compared to small nanospheres due to suppression of interband damping. In comparison to the same volume nanospheres, the examined rods showed also much weaker radiation damping. These findings explained higher light-scattering efficiencies and larger local-field enhancement factors for nanorods as compared with nanospheres; features that are especially beneficial for MEF applications.

Other authors (Novo et all 2006, Hu et all 2008) attempted to determine the optimum nanorod geometry that gives rise to the longest plasmon lifetimes by examining plasmon linewidths for nanorods of various width, but with identical aspect ratios. As expected, with the increase of the nanorod width the linewidth broadening was observed due to the increased radiation damping for larger volumes. However, such broadening was also observed for small nanorod width, due to increased surface scattering contribution. It was

found that the optimised nanorod diameter is in the range of 10-20 nm, leading to the narrowest plasmon spectra and the strongest near-field enhancements.

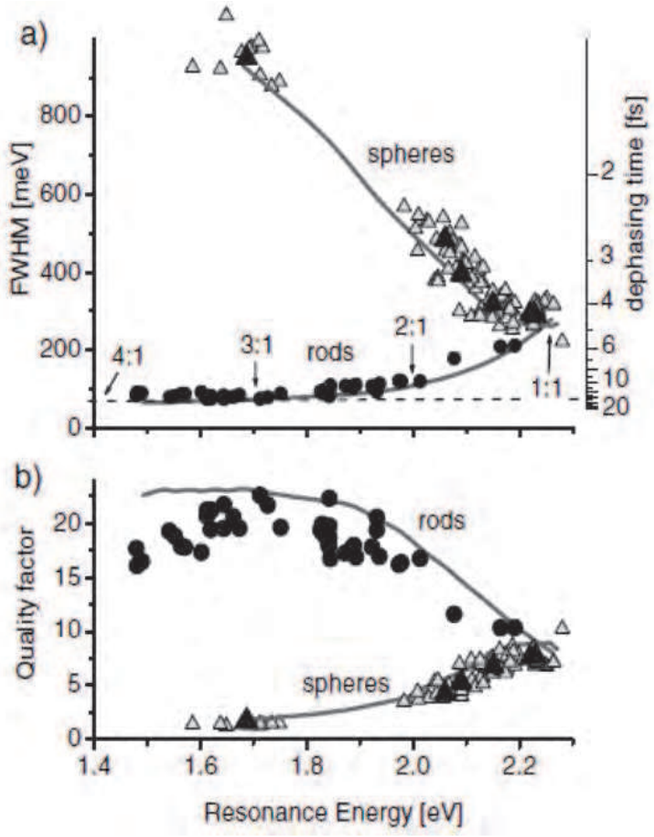

Fig. 3. (a) Measured linewidth (G) of plasmon resonances in single nanorods (dots) and nanospheres (open triangles) as a function of resonance energy E_{res}. The right scale gives the dephasing times calculated from G. Black triangles: averages for spherical particles of the same nominal size (150, 100, 80, 60, 40, and 20 nm from left to right). Lines: theoretical simulations. Some selected aspect ratios b/a are indicated in the figure. (b) The same data plotted as quality factor $Q = E_{res}/G$ which is expressed as a ratio of extinction intensity at resonance to FWHM of plasmon peak. Reprinted from Ref (Sonnichsen at all 2002).

2.3 Near field effect and coupling

Near field effect around nanoparticle depends on the particle type, size and shape. Silver is known to give more pronounced near field effects than gold due to less pronounced resonance damping by interband electron transitions, as it is known to have a higher energy separation between LSPR and interband absorption. High curvature nanoparticles give a strong field enhancement due to lightning rod-effect (Gersten 1980). Schatz and co-workers used DDA calculations (Hao et all 2004a, 2004b) to compare the electric field enhancement for nanoparticles of various shapes, showing that rods and spheroids with similar sizes and optimum aspect ratios of 3.4 produce similar enhancement in the range of $>10^3$, which are one order of magnitude larger than for spheres. The nanorod shows elevated electric fields (EF) at the ends of their long axis while the field is weakest at the centre of the rod and they were slightly higher than EF for spheroid of the same length and diameter as nanorod.

When plasmonic nanostructures are brought in close proximity to one another, their near-fields interact resulting in strong coupling. This effect was observed and most accurately quantified for electron lithographically produced gold and silver nanodisk pairs where clear trends were observed and confirmed by theoretical calculations. Coupled nanorods provide an attractive geometry, due to large oscillator strength and tunability of longitudinal plasmon mode. They were studied in various configurations: side-by-side, end-to-end and at various angles to each other (Funston et all 2009, Slaughter et all 2010). For two identical nanorods, the side-by-side geometry showed a blue-shift of the londitudinal mode and a red-shift of the transverse mode. The end-to-end geometry shows a red-shift of the longitudinal mode with a minor change in the transverse mode compared to the single nanorod spectra (see Figure 4 left). For different size nanorods arranged in the end-to-end geometry an additional antibonding dimer mode was observed on the blue side of the bonding mode peak (Figure 4 right).

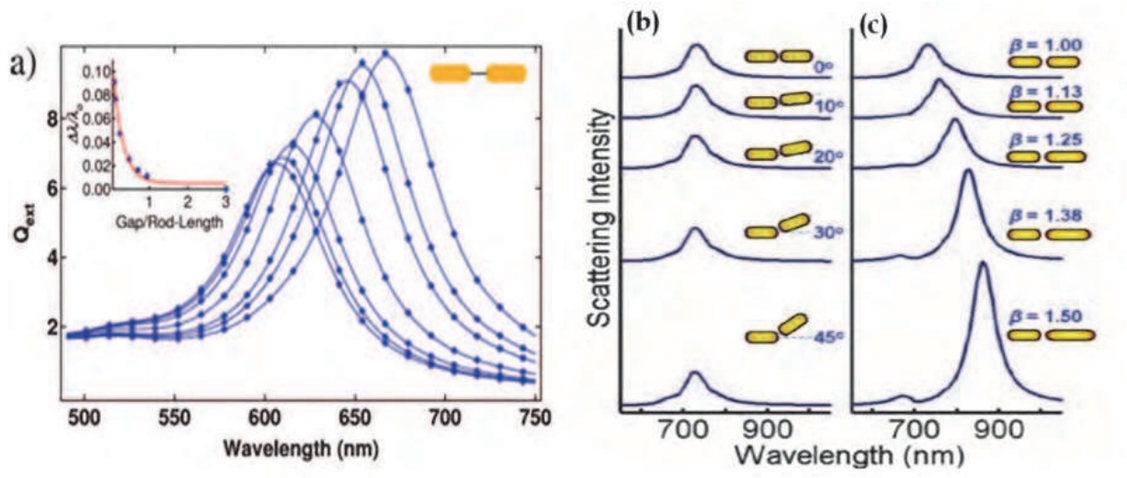

Fig. 4. Left: (a) Polarization averaged extinction of a pair of gold hemispherically capped rods with aspect ratio 2.0 interacting end-to-end as a function of interparticle separations 56.5, 42.4, 28.2, 14.1, 7.1, 5.3, and 3.5 nm with smaller separations more red shifted. Inset: Fractional shift of the longitudinal plasmon band as a function of interparticle distance scaled for rod length. The point at Gap/Rod-Length equal 3 represents the plasmon resonance of a fully decoupled rod with the same dimensions as those in the dimer. Reprinted from Ref (Funston at all 2009). Right: Integrated darkfield scattering spectra with varying angular offset for the pair of same size gold nanorods (b) and for a pair with increasing the length of the right rod starting from 80 x 30 nm in increments of 10 nm β=right rod length/left rod length (c). All spectra are normalized to the linear homo-dimer case. Reprinted from Reference (Slaughter et all 2010).

Su *et al* (Su et all 2003) demonstrated that the resonant wavelength peak of two interacting cylindrical particles is also red-shifted from that of a single particle because of near-field coupling. They found that the shift decays approximately exponentially with increasing particle spacing and becomes negligible when the gap between the two particles exceeds about 2.5 times the particle axis length. The change in plasmon position $\Delta\lambda$ in respect to plasmon position without coupling λ_0 follows a phenomenological equation:

$$\Delta\lambda/\lambda_0 = \kappa \exp^{-s/\tau D} \quad (11)$$

where κ is proportionality factor, s is the interparticle spacing, D is the diameter for cylindrical particles or length of long axis in the nanorods and τ is the decay length with the value around 0.2. This equation emphasises that $\Delta\lambda/\lambda_0$ is the same for all particles with the same s/D values. This behaviour, termed as "Universal Scaling Law", is a result of interplay of nanoparticle polarizability, which varies as the cubic power of the nanoparticle size and the plasmonic near field coupling, which varies as the inverse cubic power of the distance. It is useful to predict the coupling response from a wide variety of nanostructures. The universal scaling behaviour makes it possible to predict plasmon position shifts upon coupling between homogenous metal particles but is not able to predict the exact plasmon position or near-field strength.

3. Nanorod fabrication

3.1 Synthesis methods

Gold nanorods are most often prepared by a seed-mediated approach developed by Murphy's group in 2001 (Jana et all 2001a, 2001b, Murphy at all 2005) in which spherical 'seed' nanoparticles (4 nm diameter) are added to the growth solution containing gold salt, silver nitrate, ascorbic acid, and cetyltrimethylammonium bromide (CTAB) leading to the formation of gold nanoparticles having a rodlike morphology (Figure 5). Gold salt in the growth solution is slowly reduced in the presence of 'seed' particles while the growth-directing agent, CTAB, facilitates rod formation by preferentially binding to the side facets of the nanoparticle. The amount of silver nitrate additive is varied to alter rod length which is controlled by under-potential deposition of silver on the gold nanorod surface. Once synthesized, gold nanorod suspension is purified via centrifugation to remove excess CTAB, unreacted metal ions, and ascorbic acid. This step is important as failure to remove unreacted species will result in morphological changes over time and also to prevent cytotoxicity due to residual CTAB. The same method can be applied to produce silver nanorods. In this case the seed-mediated method uses silver 'seed' nanoparticles prepared by the reduction of silver by strong reducing agent such as sodium borohydride. Gold nanorods are very stable for all aspect ratios but low aspect ratio silver nanorods are usually unstable on the timescale of minutes in air and in light, tentatively attributed to a photo-oxidation process that releases Ag^+. However, silver nanowires that are 30 nm in diameter, but up to a dozen microns long, are very stable in these conditions.

In 2003, El-Sayed (Nikoobakt and El Sayed 2003) proposed two modifications to this method: replacing sodium citrate with a stronger CTAB stabilizer in the seed formation process and utilizing silver ions to control the aspect ratio of gold nanorods. This protocol includes two steps: 1) synthesis of seed solution by the reduction of an auric acid in the presence of CTAB with ice-cold sodium borohydride and 2) the addition of the seed solution to Au^+ stock solution in the presence of CTAB which is obtained by the reduction of $HAuCl_4$ with ascorbic acid. Silver nitrate is introduced to the gold solution before seed addition to facilitate the rod formation and to tune the aspect ratio. This method produces high yield gold nanorods (99%) with aspect ratio 1.5 to 4.5 and it avoids repetitive centrifugations. In order to grow nanorods with higher aspect ratios a co-surfactant bezyldimethylhexadecylammonium chloride (BDAC) is introduced to the original solution. By adding this surfactant it is possible to produce nanorods with aspect ratios up to 10 by changing silver concentration (Nikoobakt and El- Sayed 2003). With the Pluronic F-127 co-surfactant system nanorods with aspect ratios up to 20 were produced with good monodispersity (Iqbal et all 2007). In

both methods, the yield, monodispersity, size and fine details of gold nanorods shape are affected by multiple parameters such as seed concentration, size, structure, ascorbic acid and surfactant concentration, the use of other surfactants, additives, solvents and even the aging time.

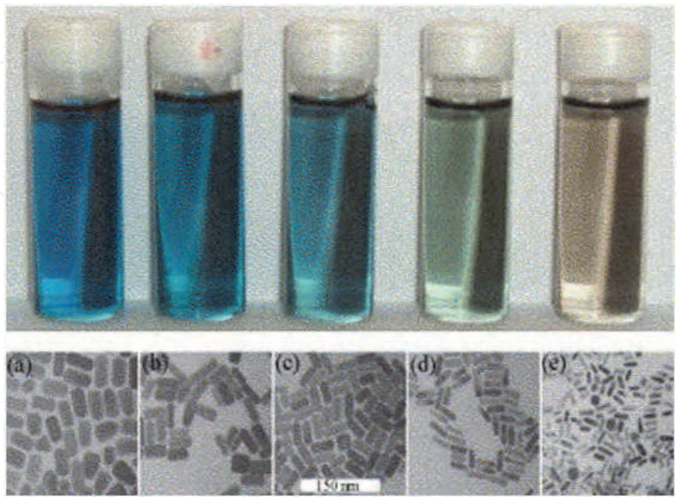

Fig. 5. The colour of gold rods and the respective micrographs. The colour changes take place for very small changes in mean aspect ratio. From Ref (Perez-Juste et all 2005).

Recently, polyol synthesis method developed by Xia and co-workers (Xia et all 2009) has been commonly used for the preparation of single-crystal Ag nanoparticles with uniform size and shape using polyvinylpyrrolidone (PVP) as a protecting agent (Willey at all 2007a, 2007b, 2005) (Figure 6). The same group synthesized Ag nanowires with higher aspects ratios by injection of ethylene glycol (EG) solutions of $AgNO_3$ and PVP, added dropwise, at a constant solution temperature of 160 °C (Chen et all 2007, Chen et all 2002). In the polyol process, the introduction of an exotic reagent is considered to be the key factor that leads to the formation of wire-like structures. In their experiments, Ag nanowires are generated using a self-seeding process and EG acts as both solvent and reducing agent, with addition of a trace amount of salt, such as NaCl, $Fe(NO)_3$, $CuCl_2$ and CuCl to assist one-dimensional growth. For the formation of silver nanowires, low precursor concentrations and slow addition rates are necessary. By controlling the injection rate, multiple-twined particle formed at the initial stage of the reduction process serve as seeds for the subsequent growth of silver nanowires. It was found that the morphologies and aspect ratios of Ag nanowires strongly depend on the molar ratio between the repeating unit of PVP and $AgNO_3$. When the molar ratio between PVP and $AgNO_3$ was more than 15, the final product was essentially composed of silver nanoparticles. When the molar ratio decreased to 6, the resulting product contained mainly nanorods. Using this method, the authors demonstrated high throughput synthesis of Ag nanorice with well controllable aspect ratios (Iqbal et all 2007) and pentagonal silver nanorods Liang et all 2009).

Other methods for gold or silver nanorod synthesis include the electrochemical method (Pietrobon et all 2009, Goldys et all 2007) in which nanorods are grown in an electrolytic solution between two electrodes under controlled currents or template based methods (e.g. synthesis of particles confined within cylindrical membrane pores or synthesized around cylindrical particles). Template-related approaches have been performed with porous

anodic aluminum oxide membranes, carbon nanotubes or block copolymers (Nicewarner-Pena et all 2001). Other advanced fabrication methods such as electron-beam lithography (EBL) were also used to achieve high level of control over shape, position and arrangement of gold or silver nanorod structures (Yu at all 1997, Smythe et all 2007, Billot et all 2006). Assemblies of nanorods with long axis of the nanorods protruding from substrate were also obtained by oblique angle vacuum evaporation (Chaney et all 2005, Liu et all 2006). Examples of synthesised silver and gold nanorods are shown in Figure 5 and Figure 6.

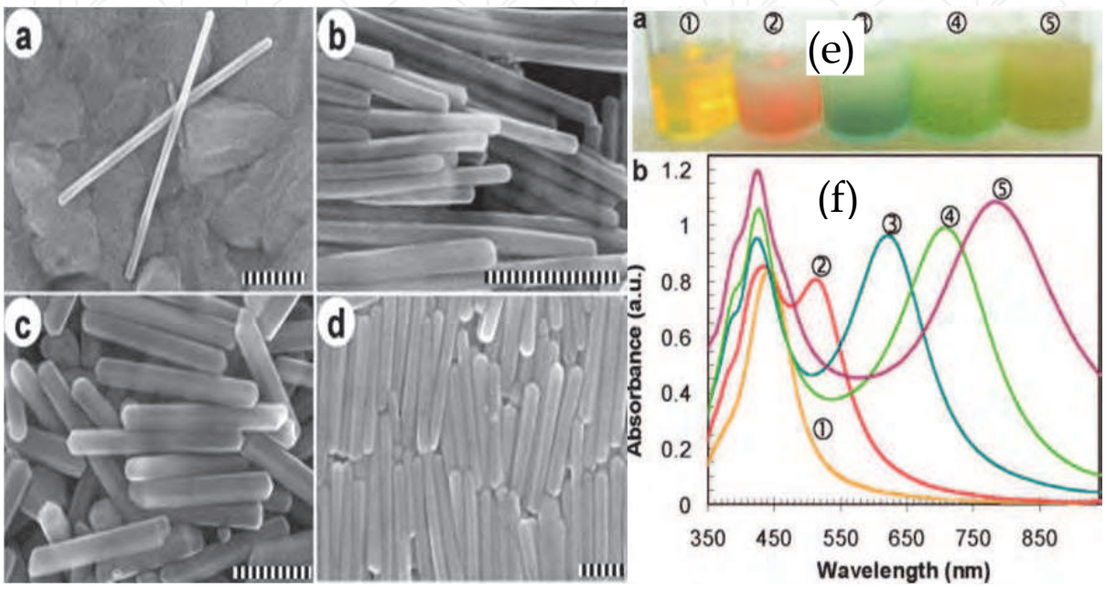

Fig. 6. Left: SEM images of longer pentagonal faceted silver nanorods with the aspect ratios of (a) 8.7 and (b) 10.2; as well as (c) and (d) longer 2μm pentagonal faceted silver rods regrown from ca. 0.5 μm rods. The scale bar is 100 nm for (a) and (b) and 2 μm for (c) and (d). Right: Optical properties of synthesized pentagonal faceted silver nanorods. (e) Photographs of aqueous dispersions and (f) UV-vis spectra of pentagonal faceted silver nanorods with thickness of 49.5 ± 2.5 nm and length of (1) 62 ± 3 nm; (2) 75 3± nm; (3) 108 ± 5 nm; (4)142 7± nm; (5) 158 ± 8 nm. From Ref (Pietrobon et all 2009).

3.2 Surface modification

Introduction of surface modification makes it possible to increase stability, facilitate surface chemistry, tune plasmonic properties and broaden practical applications of metal nanorods. For instance, by introducing silver coating on gold nanorods surface it is possible to increase metal enhanced fluorescence due to reduced plasmon damping and to provide a broader spectral range by controlling plasmon peak position. Silica coating can be used to control spacing from the metal surface, it prevents quenching due to FRET and induces red-shift of plasmon resonance position. Silver over-coating is usually carried out by the reduction of silver nitrate with ascorbic acid at base condition in the presence of gold nanorods and a stabilizing agent such as citrate, CTAB and PVP and the silver thickness is controlled by tuning the concentration of silver precursor. Silicon coatings are produced on silver or gold nanorods by dispersing nanorods in solution with 3-mercaptopropyl trimethoxysilane (MPTMS) or 3 mercaptopropyl triethoxysilane (MPTES) and adding aqueous sodium silicate (Obare et all 2001).

3.3 Bioconjugation

Biological detection methods based on fluorescence require controlled, specific binding protocols in which signal from fluorescent dye attached to signalling molecule is measured and quantified. To take advantage of the effect of MEF the biological molecule with fluorophore is either attached directly to the nanostructured metal surface or through another molecule using highly specific binding protocols. There is also a fast, growing interest in using gold nanorods in imaging applications of cells in both in vivo and in vitro due to their exceptional light scattering properties and relatively intense two-photon luminescence (Mohamed et all 2000).

One of the reasons that MEF has not been intensely explored for colloidal silver or gold nanorods is the fact that during their synthesis complex organic molecules such as CTAB or PVP remain on their surface and these molecules are not suitable for biological binding protocols without exchange or complex modifications. Conjugation of biomolecules to gold or silver nanorods can be divided into four different methodologies: direct ligand exchange, the use of biofunctional linker, surface coating and electrostatic absorption. Similarly to other types of gold or silver nanoparticles, thiol exchange is the most common way to replace the capping molecules, since the metal–sulfur bond is known to be stronger than bonds with alternative functional groups (i.e., amines, carboxylic acids, alcohols, and phosphors). Molecules, such as PEG (Grand et all 2003), DNA (Niidome et all 2006), or lipids (Yelin et all 2003) are firstly functionalized with an alkythiolated linker and then bound to gold nanorods through Au–S bonds in a prolonged (few hours) reaction. For complete exchange, sonication and heating might be required to remove CTAB while preventing the nanoparticles from aggregation. For some biomolecules, such as antibodies and proteins, thiolation is complicated by the fact that molecules are too large to reach the gold surface due to dense packing of the CTAB double layers. In this case, small biofunctional molecules such as 3-mercaptopropionic acid (MPA), 11-mercaptoundecanoic acids (MUDA) (Brown et all 2001, Dai et all 2008) and cysteamine (Li et all 2006) are suitable replacements. As most thiol molecules are not water-soluble, the use of organic solvents (such as ethanol and chloroform) and phase extraction are needed. This presents challenges for the modification of gold or silver nanorods as they easily aggregate in organic solvents. The easiest way to prevent this aggregation is to adsorb charged proteins, such as antibodies, by electrostatic forces. At pH higher than the isoelectric point (pI), the proteins are negatively charged, and therefore they can be directly adsorbed to metal nanorods via electrostatic attraction. However, the protein/rod ratio needs be optimized to avoid the aggregation of the nanoparticles due to charge neutralization while ensuring high loading of the protein onto the nanorods.

Despite the fact that gold and silver nanorods produced by seed mediated methods are characterized by the most controllable and tunable LSPRs, more work is required to demonstrate their full potential for metal enhanced fluorescence.

4. Experimental examples of MEF on metal nanorods

Since the synthesis of gold nanorods with decent yield and monodispersity has been developed comparatively recently, only a few papers were published related to their application in MEF. Up to date, the majority of biological applications of metal nanorods is based on direct observation of changes in position of plasmon resonances upon binding with molecules, which can involve agglomeration, binding in end-to-end pairs or release of

molecules which fluorescence is otherwise quenched, or in imaging applications, utilizing their strong anisotropic light scattering properties. Imaging applications often use dark field microscopy to improve contrast and take advantage of excellent scattering properties of metal nanoparticles. As the scattering cross-section of gold nanoparticles is very high, they offer better visibility than fluorescent dye molecules and are therefore very well suited for biomedical imaging using reflectance confocal microscopy and for in vivo imaging using optical coherence microscopy. In the case of white light illumination using simple dark field microscopy, which is suitable for cellular imaging, the particles scatter strongly around the spectral position of surface plasmon resonance making them individually recognizable by their colour that is dependent on the particle size and shape. Applications involving modifications of fluorophore emissions in close proximity to metal nanorods are just only starting to appear in literature due to limitations in commercial availability of metal nanorods with functionalized surfaces for biological conjugations.

4.1 Polarisation dependence

The geometry of nanowires and nanorods is clearly compatible with strong polarisation effects, and it is therefore surprising that this property in MEF has only just been demonstrated by Ming et *al*. (Ming et all 2009). This group described strong excitation polarization dependence of the plasmon-enhanced fluorescence on single gold nanorods. The nanorods were encapsulated in a thin ~ 20 nm silica shell, while the nanorods were about 90 nm long and 42 nm wide, with an aspect ratio of ~ 2.1. The authors showed that fluorescence from the organic fluorophores (Oxazine 725 perchlorate) embedded in a mesostructured silica shell around individual gold nanorods is enhanced by the longitudinal plasmon resonance of the nanorods. This enhancement is the greatest (by a factor of 56) when the excitation energy is matched to the longitudinal plasmon energy. The polarization dependence of the plasmon-enhanced fluorescence is due to the dependence of the averaged electric field intensity enhancement within the silica shell on the polarisation of the excitation beam. Under off-resonance excitation, the electric field intensity contour around a nanorod rotates away from the length axis as the excitation polarization is varied. As expected, the fluorescence enhancement factor increases as the longitudinal plasmon wavelength is tuned close to the excitation wavelength by varying nanorod length. Furthermore, the emission spectrum of the fluorophore is modified by the longitudinal plasmon resonance of the gold nanorods, a phenomenon attributed to the enhanced probability of fluorophore transition from the excited state to a specific vibrational ground state with the transition energy close to the plasmon resonance energy. The authors did not consider the possibility of strong coupling between fluorophores and plasmons, which is also able to produce similar spectral deformations. A linear correlation between the modified emission peak wavelength and the longitudinal plasmon wavelength was observed.

4.2 Complex nanowire geometries.

It is not necessary for nanorods or nanowires to have uniform shapes in order to show attractive optical properties. Any elongated shape is capable of similar pattern of fluorescence enhancement as long as there is adequate electrical contact between nanowire subsections. This has been illustrated in the publication of He and Zhao (He and Zhao 2009). In this work novel silver chain-like triangular nanoplate assemblies (CTNAs) were synthesized via a solvothermal approach. The shape of CTNAs was determined by synthesis

parameters, including the concentration of PVP, reaction time and temperature. Each CTNA is a combination of one dimensional nanobelt and two-dimensional nanoplates. The edges of the nanoplates in the assembly are parallel to each other in order to lower surface energy. Interestingly, this novel nanostructure is able to show high enhancement factors in metal-enhanced fluorescence. Typically, 88- and 13-fold enhancement in the emission intensity of dye Rhodamine B were, respectively, achieved on the surface of silver colloids and silver coated-glass. The silver nanostructures were coated with PVP to ensure nanoscale separation between the metal and fluorophores. Our own studies (Goldys et all 2007) showed that electrochemically deposited silver structures with nanowires of 50−100 nm in diameter demonstrated high up to 57 times fluorescence amplification of conjugated to HSA protein, FITC fluorophore and strongly reduced fluorescence lifetimes. Both quantities depended on the structure thickness. With increasing thickness of the silver nanostructure the fluorescence amplification proportionally increased in correlation with strongly reduced fluorophore lifetimes. This thickness dependence was caused by fluorophore interaction with plasmon excitations in coupled nanowires extending over micrometer size regions. Thus the amplification was attributed to a combination of extended structure area and strong plasmonic coupling between nanowires which also helped to radiatively scatter via lighting rod effect the fluorescence emission. Another system (Drozdowicz-Tomsia et all 2010) investigated in our group contained complex elongated silver fractal nanostructures grown on silicon. Fluorescence of Deep Purple fluorophore in this structure showed uniform enhancements (average factor of 40) dominated by emission enhancement, and this was achieved by good correlation of fluorophore emission with plasmon position for such system.

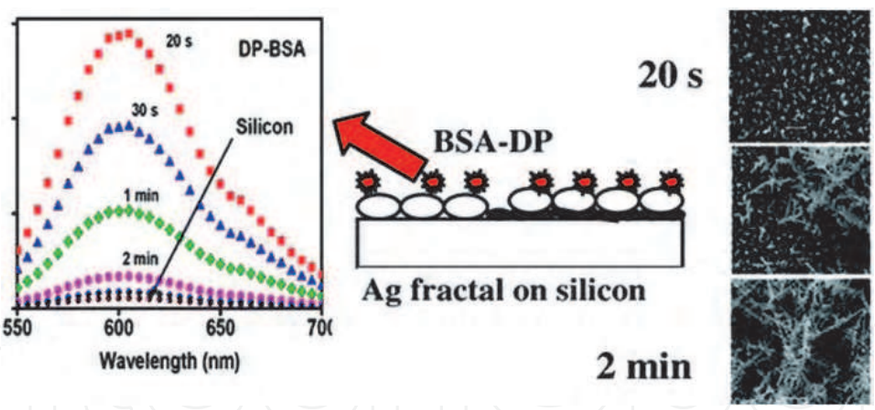

Fig. 7. Fluorescence enhancement study of BSA-Deep Purple (DP) fluorophore conjugate on silver fractal deposited by electroless deposition on silicon. Left: fluorescence spectra of DP for various silver growth times, middle: schematic of experimental sample, right: SEM images of silver fractals at various growth times. Reproduced from Ref (Drozdowicz-Tomsia et all 2010).

4.3 Nanorod-modified surfaces

The advantage of columnar geometry with nanorods coating the surface was realised as early as 2005 with the work by Aslan et al (Aslan et all 2005) who attempted to create a fast an inexpensive method of metal surface modification that would show at least some advantages of nanolithography. They developed two new techniques for the deposition of

silver nanorods onto conventional glass substrates. In the first method, silver nanorods were deposited onto 3-(aminopropyl)triethoxysilane (APTMS)-coated glass substrates simply by immersing the substrates in the silver nanorod solution. In the second method, spherical silver seeds that were chemically attached to the surface were subsequently converted and grown into silver nanorods in the presence of a cationic surfactant and silver ions. The size of the silver nanorods, ranging from tens of nanometers to a few micrometers, was controlled by sequential immersion of silver seed-coated glass substrates into the growth solution and by the duration of immersion. Atomic force microscopy and optical density measurements showed that the silver nanorods deposited onto the surface of the glass substrates were irregularly deposited. These new surfaces have been applied to MEF where they performed much better compared to traditional silver islands or colloid films, with amplification factors between 10 and 50.

The same idea has been explored in a more recent publication from Halas group (Bardhan et all 2009) who enhanced fluroescence of an infrared dye IR800 with gold nanorods and nanoshells. Fluorescent molecules emitting at wavelengths in the physiologically relevant "water window" (700-900 nm) are of particular interest due to large penetration depth of near infrared (NIR) light in most biological media and offer the potential for imaging at significant depths in living tissues. However, achieving bright fluorescent emission with photostable and biocompatible near-IR fluorophores has proven to be extremely difficult, prior to this work. Several interdependent processes are responsible for IR800 fluorescence enhancement, these include absorption enhancement, scattering enhancement, and radiative decay rate enhancement. In this report, the scattering efficiency of a nanoparticle appeared to provide the most important mechanism for improving the quantum yield of a fluorophore. Nanorods preferentially enhance the emission of the fluorophore by absorption enhancement, owing to the high-intensity near field resulting from the longitudinal plasmon resonance. However, due to the significant difference in scattering cross sections of nanoshells and nanorods, it is apparent that nanoshells increase the coupling efficiency of the fluorescence emission to the far field more efficiently than nanorods. This explains the 40-fold fluorescence enhancement observed for IR800 bound to nanoshells compared to the 9-fold enhancement for IR800 bound to nanorods. The radiative decay rate enhancement of the fluorophore is dependent on both the scattering efficiency as well as the absorption efficiency of nanoparticles. This explains why nanorods enhance the quantum yield of IR800 by 74% as well as considerably decrease the fluorophore's lifetime.

4.4 Applications of nanorods in SERS

Surface-deposited nanorods have also been tested with respect to their surface-enhanced Raman scattering (SERS) properties (Guo et all 2009). These authors established the correlation of the shape andposition of surface plasmon resonance with SERS properties of gold nanorods in dilute colloids. A series of gold nanorods with various aspect ratios was prepared via an improved seed-mediated technique. As discussed previously, increasing the aspect ratio finely tunes the position of the longitudinal plasmon mode of the nanorods in a wide spectral range. The subtle influence of surface plasmon resonance on SERS was then demonstrated by gradually tuning the plasmon wavelength across a fixed excitation line. The authors demonstrated that close overlap of surface plasmon and the excitation line maximizes the SERS enhancement. Tao et al. (Tao et all 2003) have earlier attempted to create a similar SERS surface by using a Langmuir-Blodgett method for silver nanorod

deposition. They assembled large area (over 20 cm^2) monolayers of aligned silver nanowires that were 50 nm in diameter and 2-3 um in length. Their nanowires had pentagonal cross-sections and pyramidal tips. They were close-packed and aligned parallel to each other. The resulting monolayers deposited on nanowires were tested for SERS with electromagnetic field enhancement factors of $2x10^5$ for thiol and 2,4-dinitrotoluene, and 2×10^9 for Rhodamine 6G. Another example are the studies by Oyelere et al. (Oyelere et all 2007) who used nanorods to observe enhanced Raman bands from the nucleus of both cancer and non-cancer cells. In this study, the nucleus localization signal from binding peptide was conjugated to gold nanorods via a thioazide linker, and the incubation of the conjugates with cells led to preferential accumulation of the nanorods inside the cellular nucleus. Using a micro-Raman spectrometer with excitation at 785 nm, DNA backbone vibration and guanine Raman bands from a single cell were clearly observed. Normal and cancer cells showed fingerprint differences which could be useful for molecular cancer diagnosis. In the recent studies by Huang et al. (Hunag et all 2007) the assembly of gold nanorods by cancer cells due to the binding of the anti-EGFR-conjugated rods to the over-expressed EGFR (epidermal growth factor receptor) on the cancer cell surface has given highly enhanced, sharp, and polarized SERS, while no SERS was observed from the majority of the normal cells.

4.5 Applications of nanorods for resonant energy transfer

While metal nanostrutcures are known to extend the range of resoanant energy transfer, there is very limited literature on the application of nanorods. Zhou et al. (Zhou et all 2010) reported efficient plasmon-mediated excitation energy transfer between the CdSe/ZnS semiconductor quantum dots (QDs) across silver nanorods array consisting of nanorods with lengths up to 560 nm. The sub-wavelength imaging and spectral response of the silver nanowire arrays with near-field point-source excitations have been also theoretically simulated. This nanowire array showed efficient exciton-plasmon conversion at the input side of the array through strong near-field coupling, directional guiding of waves and resonant transmission *via* half-wave plasmon modes of the nanowire array, making possible sub-wavelength imaging at the output side of the array. These advantages allow a long-range radiative excitation energy transfer with a high efficiency and good directionality.

4.6 Nanowires on metal films

A number of recent works have been focusing on using metal nanowires with a columnar morphology protruding from metal films. These films have been produced by using oblique angle deposition (OAD) technique. (Latakhia and Messier 2005, Messier and Latakhia 1999). The growth mechanism is based on self-organized nucleation of nanoparticles and subsequent highly directional growth due to atomic shadowing of the nanoparticle flux reaching the substrate at a large, oblique angle with respect to the substrate normal. The OAD substrates have been recently used for surface enhanced Raman effect for virus detection (Shanmukh et all 2006). The application in MEF has been demonstrated only recently (Abdulhalim et all 2009). In this work metal enhanced fluorescence from porous, metallic sculptured thin films was demonstrated for sensing of bacteria in water. Enhancement factors larger than 15 were observed using structures made of silver, aluminium, gold, and copper with respect to their dense film counterparts. The structures used are assemblies of tilted, shaped, parallel nanowires prepared with

several variants of the oblique-angle-deposition technique. Comparison between the different films indicates that the enhancement factor is higher when the tilt is either small (30 deg) or large (80 deg); thus, the enhancement is higher when only a single resonance in the nanowires is excited.
Several mechanisms can contribute to the MEF from metallic OAD substrate, firstly such structures can act as reflective interfaces, secondly they constitute a porous material with high surface-to-volume ratio, and finally, metal nanorods enhance the local electromagnetic field and act as nanoantennas. The dipole-dipole coupling between neighbouring nanorods is also expected to play a role. The dipole-dipole interaction occurs when light incident on a nanorod induces across it an electric field that depends both on the shape of the nanorod and on the contributions from the neighboring nanorods. Near-field effects are important for internanorod distance much less than the wavelength while far-field effects can play a role for nanorods of larger size.

4.7 Single nanorods and MEF

Recently, Fu, Zhang and Lakowicz (Fu et all 2010) used a single nanorod to enhance emission of fluorophore molecules coupled to one of its ends. Through covalent linkages of fluorophores at the preferred longitudinal axis of the nanorods, they were able to increase the overall optical signal for improved sensitivity. Their nanorods had an average aspect ratio of 6 (ca. 80 nm in length and 13 nm in diameter) and the longitudinal plasmon band at 980 nm. Functionalization of the nanorods was performed with biotin, however only on rod ends, owing to the difficulty of replacing CTAB molecules on the sides of the nanorods. Binding of thiol molecules to the end of the gold nanorod tips was mediated by streptavidin. The functionalized nanorods were incubated with a low concentration of solution of oligonucleotides labelled with biotin and Cy5 (Biotin- 3′-AGG-TGT-ATG-ACC-GGT-AGA-AG-5′-Cy5, ca. 8 nm in length) to obtain hybrid nanocomplexes. This linker molecule has been optimisted for best fluorescence enhancement. Much higher fluorophore emission rate has been clearly observed, approximately 40-fold greater than that observed in the absence of gold nanostructure. Additionally, polarization dependence of the excitation was demonstrated on a single Au nanocomplex excited at different directions. The emission intensity decreased abruptly as the excitation angle rotated 90° as for this orientation transverse plasmon excitations were excited in gold nanorods. These occur at much shorter wavelengths and out of resonance with fluorophore excitation/emission. The magnitude of the enhancement also depends on the location of the fluorophore around the particle and the orientation of its dipole moment relative to the metallic surface.

5. Theoretical simulations

Theoretical simulations of spontaneous emission of fluorophores coupled to nanoantennas were carried out by Giannini et al. (Giannini et all 2009). The modification of the corresponding radiative and nonradiative decay rates and resulting quantum efficiencies was calculated by means of the rigorous formulation of the Green's theorem surface integral equations. Resonant enhancement of the radiative and nonradiative decay rates of a fluorescent molecule was shown when coupled to an optical dimer nanoantenna. A numerical example was presented comprising two silver rectangular nanowires with the dimensions of each rectangle 20 x 200 nm, with a gap of 10 nm. Upon varying the dipole

position, it was possible to obtain preferential enhancement of radiative decay rates over the nonradiative counterpart, resulting in an increase of the internal quantum efficiency. For emitters positioned in the gap, quantum efficiency enhancements from the initial value of 1% to 75% was possible, however emitters that are originally more efficient can not be enhanced as much.

Kappeller *et al* (Keppeler et all 2007) studied locally enhanced optical fields created near tunable laser-irradiated metal nanostructures acting as local probes. Using three dimensional simulations with a commercial COMSOL Multiphysics software package based on the finite element method (FEM) they have shown electromagnetic fields near various optical antennas and optimized their geometry in order to obtain a strong enhancement in a selected frequency range and the results are shown in Figure 8 below. They compared three antenna designs: a) a self-similar antenna, which is consisting, of four overlapping gold nanospheres each smaller than the previous by scaling constant with tip of 10 nm radius, b) conical antenna, which has the same length and outside front and end curvatures as previous antenna and c) nanorod antenna, which has 200 nm length and 20 nm diameter.

According to their calculations the strongest lighting rod effect was observed for self-similar antenna, slightly weaker for conical antenna and the most complex for nanorod antenna where bright and dark modes were observed at different spectral resonance conditions. This suggests that strong lighting rod effect desirable for MEF can be achieved when the length of the nanorods is carefully tuned to emission of fluorophore.

6. Conclusions

Silver and gold nanorods have shown excellent optical properties suitable for a wide range of applications including MEF, SERS and resonant energy transfer. In this chapter we outlined the basic theory of optical properties of the nanorods, centred around their polarisability. We highlighted the opportunities they provide to tune plasmonic properties by varying the details of nanorod shape and size. For MEF applications the key parameters of relevance are the match of fluorophore emission and excitation to plasmonic characteristics, because at these wavelengths the near-field enhancement of the electromagnetic fields are maximised. The plasmon linewidth and plasmon dephasing time are also relevant as long dephasing times lead to increased fields. The effect of inter-particle coupling can also be exploited to maximise MEF, as well as the fact that complex geometries for example nanorods on a metal film may provide not only improved plasmon coupling but also better fluorescence out-coupling efficiency and high surface areas. Polarisation properties of aligned nanorods have been reported, but are yet to be exploited more fully. Theoretical work in this area is facilitated by the availability of commercial software packages such as COMSOL Multiphysics, but those attempting to use them should carefully match the simulated results with experiments, which still present a challenge. Further challenges remain in the areas of nanorod synthesis and post-processing discussed in the second part of this chapter. These include the understanding of nanorods chemistry, their functionalisation, controllable assembly and stability. Despite this (or perhaps because of this) we expect this area to continue rapid progress, stimulated by the increasing commercial availability of nanorods including their bioconjugates and a wide range of significant applications in biosensing and bioimaging.

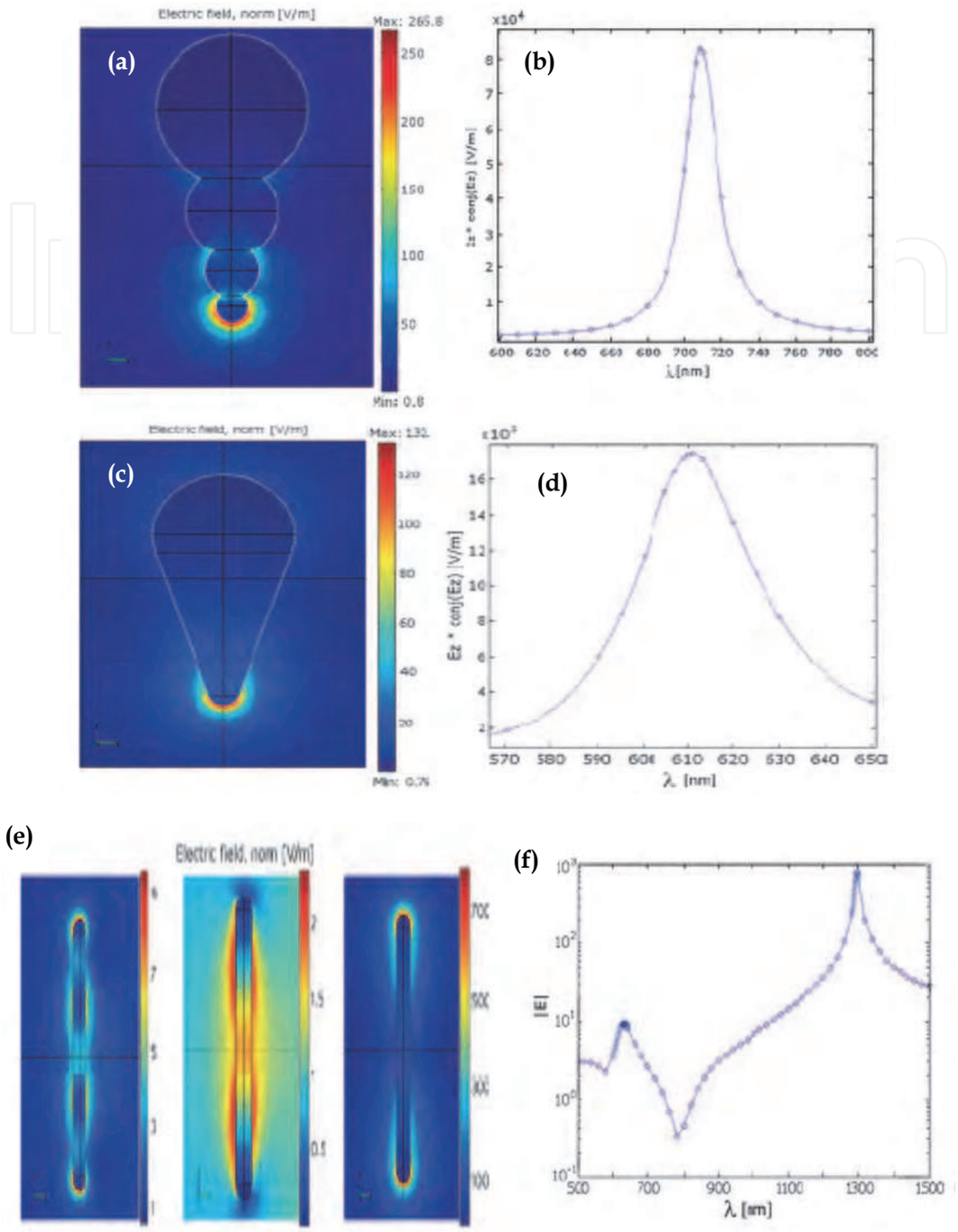

Fig. 8. Left: calculated field strength (|E|) for the resonance conditions and right: corresponding resonance spectra for three different antenna designs: (a) self-similar antenna at resonance λ= 708 nm, (c) conical antenna with resonance at 610 nm, (e) nanorod antenna with field distributions corresponding to the three extrema observed in resonance curve (f). For nanorod antenna electric field distribution (e) at λ~1300 nm (right) corresponds to the λ/2 mode, the mode at λ~650 nm (left) is the 3/2 λ mode and the 'dark' mode at λ~780 nm (centre) corresponds to the symmetric λ-mode. (Reproduced from Ref Keppeler et all 2007).

7. References

Abdulhalim I.; Karabchevsky A.; Patzig C.; Rauschenbach B.; Fuhrmann B.; Eltzov E.; Marks R, Xu J., Zhang F.; and Lakhtakia A.; (2009) "Surface enhanced fluorescence form metal-sculptured thin films with application to biosensing in water" *App. Phys. Lett.*, 94, 063106.

Aslan K.; Leonenko Z.; Lakowicz J. R.; and Geddes C. D.; (2005) "Fast and Slow Deposition of Silver Nanorods on Planar Surfaces: Application to Metal-Enhanced Fluorescence", *J. Phys. Chem. B*, 109, 3157-3162

Bardhan R.; Grady N. K.; Cole J. R.; Joshi A.; and Halas N.J.; (2009) "Fluorescence Enhancement by Au Nanostructures: Nanoshells and Nanorods", *ACS Nano*, , 3, 744-752.

Billot L.; Lamy de la Chapelle M.; Grimault A.-S.; Vial A.; Barchiesi D.; Bijeon J.-L.; Adam P.-M.; Royer P.; (2006) "Surface enhanced Raman scattering on gold nanowire arrays: Evidence of strong multipolar surface plasmon resonance enhancement" *Chem. Phys. Lett.*, 422, 303.

Brown M.D.; Schatzlein A. G.; and Uchegbu I.F.; (2001) "Gene delivery with synthetic (non viral) carriers". *Int. J. Pharm.*, 229, 1–21.

Chaney S. B.; Shanmukh S.; Dluhy R. A.; and Zhao Y. P.; (2005) "Aligned silver nanorod arrays produce high sensitivity surface-enhanced Raman spectroscopy substrates," *Appl. Phys. Lett*, 87, 031908.

Chen Y.; Munechika K.; and Ginger D S.; (2007) "Dependence of Fluorescence Intensity on the Spectral Overlap between Fluorophores and Plasmon Resonant Single Silver Nanoparticles" *NanoLetters* 7, 690-696.

Chen, J. Y.; Wiley, B. J.; & Xia, Y. N.; (2002) "One-dimensional nanostructures of metals: Large-scale synthesis and some potential applications". *Langmuir,* 2007, 23, 4120-4129 (b) Sun, Y. G. & Xia, Y. N. "Large-scale synthesis of uniform silver nanowires through a soft, self-seeding, polyol process". *Advanced Materials*, 14, 833-837.

Corrigan, T. D.; Guo, S. H.; Szmacinski, H.; Phaneuf, R. J.; (2006) "Systematic study of the size and spacing dependence of Ag nanoparticle enhanced fluorescence using electron-beam lithography" *Appl.Phys. Lett.*, *88* (10), 101112.

Corrigan, T. D.; Guo, S.; Phaneuf, R. J.; Szmacinski, H.; (2005) "Enhanced Fluorescence from Periodic Arrays of Silver Nanoparticles" *J. Fluoresc.*, *15* (5), 777–784.

Dai, Q.; Coutts, J.; Zou, J.; Huo, Q.; (2008) "Surface modification of gold nanorods through a place exchange reaction inside an anionic exchange resin". *Chem. Comm.* 2858-2860.

Drozdowicz-Tomsia K.; Xie F.; Goldys E.M.; (2010) "Deposition of silver dentritic nanostructures on silicon for enhanced fluorescence" *J Phys Chem C*, 114, 1562-1569

Felidi, N.; Aubard, J.; Levi, G.; (1999) "Discrete dipole approximation for ultraviolet–visible extinction spectra simulation of silver and gold colloids" *J. Chem. Phys. 111* (3), 1195–1208.

Fu Y.; Zhang J.; and Lakowicz J. R.; (2010) "Plasmon-Enhanced Fluorescence from Single Fluorophores End-Linked to Gold Nanorods", *J. Am. Chem. Soc. 132*, 5540–5541

Funston A. F.; Novo C.; Davis T. J.; Mulvaney P. (2009), "Plasmon Coupling of Gold Nanorods at Short Distances and in Different Geometries" *NanoLett.*, 9, 1651-1658.

Gans R, (1915) "Über die Form ultramikroskopischer Silberteilchen" *Ann. Phys.*, 47, 270.

Geddes, C. D.; Cao, H.; Gryczynski, I.; Gryczynski, Z.; Fang, J. Y.; Lakowicz, J. R.; (2003) "Metal-Enhanced Fluorescence (MEF) Due to Silver Colloids on a Planar Surface:

Potential Applications of Indocyanine Green to in Vivo Imaging" *J. Phys. Chem. A*, *107* (18), 3443–3449.

Geddes C. D.; Parfenov A.; Roll D.; Gryczynski I.; Malicka J.; Lakowicz J. R.; (2003) "Silver fractal-like structures for metal-enhanced fluorescence: Enhanced fluorescence intensities and increased probe photostabilities". *J. Fluorescence*, *13*, 267-276.

Gersten, J. I.; Nitzan A.; (1985) "Photophysics and photochemistry near surfaces and small particles" *Surf. Sci* 158, 165.

Giannini V.; Sánchez-Gil J. A.; Muskens O. L.; and Rivas J. G.; (2009) "Electrodynamic calculations of spontaneous emission coupled to metal nanostructures of arbitrary shape: nanoantenna-enhanced fluorescence", *J. Opt. Soc Am. B*. 26, 1569-1577.

Goldys,E. M,; Drozdowicz-Tomsia,K,; Xie, F, Shtoyko, T.; Matveeva, E.; Gryczynski, I.; and Gryczynski Z.; (2007) "Fluorescence amplification by electrochemically deposited silver nanowires with fractal architecture" *J. Am. Chem. Soc.*, *129* (40), pp 12117–12122.

Grand J.; Kostcheev S.; Bijeon J.-L.; Lamy de la Chapelle M.; Adam P.-M.; Rumyantseva A.; Le´rondel G.; Royer P.; (2003) "Optimization of SERS-active substrates for near-field Raman spectroscopy" *Synth. Met.* 139, 621.

Guo, S. H.; Tsai, S. J.; Kan, H. C.; Tsai, D. H.; Zachariah, M. R.; Phaneuf, R. J.; (2008a) "The Effect of an Active Substrate on Nanoparticle-Enhanced Fluorescence" *Adv. Mater*. 20, 1424–1428.

Guo, S. H.; Tsai, S. J.; Kan, H. C.; Tsai, D. H.; Zachariah, M. R.; Phaneuf, R. J. (2008b) "Spacer Layer Effect in Fluorescence Enhancement from Silver Nanowires over a Silver Film; Switching of Optimum Polarization" *Adv. Mater. 20* (8), 1424–1428.

Guo H.; Ruan F.; Lu L.; Hu J.; Pan J.; Yang Z.; and Ren B.; (2009) "Correlating the Shape, Surface Plasmon Resonance, and Surface-Enhanced Raman Scattering of Gold Nanorods", *J. Phys. Chem. C 113,* 10459–10464

Hao, E.; Schatz, G. C.; (2004) "Electromagnetic field around silver nanoparticles and dimmers" *J. Chem. Phys. 120*, 357-366.

He X.; Zhao X.; (2009) "Solvothermal synthesis and formation mechanism of chain-like triangular silver nanoplate assemblies: Application to metal-enhanced fluorescence (MEF)", *Applied Surface Science* 255, 7361–7368

Hu M.; Novo C.; Funston A.; Wang H.; Staleva H.; Zou S.; Mulvaney P.; Xia Y.; Hartland G.V.; (2008) "Dark-Field Microscopy Studies of Single Metal Nanoparticles: Understanding the Factors that Influence the Linewidth of the Localized Surface Plasmon Resonance" *J. Mater. Chem*. 18, 1949.

Huang X.; Neretina S.; and El-Sayed M.A.; (2009) "Gold Nanorods: From Synthesis and Properties to Biological and Biomedical Applications" *Adv. Mater*. 21, 4880–4910.

Huang X.; El-Sayed I. H.; Qian w.; El-Sayed M. A.; (2007) "Cancer Cells Assemble and Align Gold Nanorods Conjugated to Antibodies to Produce Highly Enhanced, Sharp, and Polarized Surface Raman Spectra: A Potential Cancer Diagnostic Marker" *Nano Lett.* 7, 1591.

Hutter E.; Fendler J. H.; (2004) "Exploitation of Localized Plasmon Resonance Adv. Mat. 16, 1685-1706.

Iqbal M.; Chung Y.; Tae G.; (2007) "An enhanced synthesis of gold nanorods by the addition of Pluronic (F-127) *via* a seed mediated growth process" *J. Mater. Chem.* 17, 335-342.

Jana N. R.; Gearheart L.; Murphy C. J.; (2001) "Seed-mediated growth approach for shape-controlled synthesis of spheroidal and rod-like gold nanoparticles using a surfactant template" *Adv. Mater.* 13, 1389.

Jana N. R.; Gearheart L.; Murphy C. J.; (2001) "Wet Chemical Synthesis of High Aspect Ratio Cylindrical Gold Nanorods" *J. Phys. Chem. B* 105, 4065.

Jensen, T. R.; Malinsky, M. D.; Haynes, C. L.; Van Duyne, R. P. (2000) "Nanosphere Lithography: Tunable Localized Surface Plasmon Resonance Spectra of Silver Nanoparticles" *J.Phys. Chem. B 104* (45), 10549–10556.

Kappeler R.; Erni D.; Xudong C.; and Novotny L.; (2007) "Field Computations of Optical Antennas", *J. Comp. Theor. Nanosc. 4, 686.*

Kelly K.L.; Coronado E.; Zhao L.L.; and Schatz G.C.; (2003) "The Optical Properties of Metal Nanoparticles: The Influence of Size, Shape, and Dielectric Environment" *J. Phys. Chem. B* 107, 668.

Kerker, M.; Blatchford, C. G.; (1982) "Elastic scattering, absorption, and surface-enhanced Raman scattering by concentric spheres comprised of a metallic and a dielectric region" Phys. Rev. B 26, 4082.

Khlebtsov B. N.; Khlebtsov N. G.; (2007) "Multipole Plasmons in Metal Nanorods: Scaling Properties and Dependence on Particle Size, Shape, Orientation, and Dielectric Environment" *J. Phys. Chem. C 111,* 11516-11527.

Kummerlen, J.; Leitner, A.; Brunner, H.; Aussenegg, F. R.; Wokaun, A.; (1993) "Enhanced dye fluorescence over silver island films: Analysis of the distance dependence" .*Mol. Phys. 80* (5), 1031–1046.

Lakhtakia A.; and Messier R.; (2005) "Sculptured Thin Films: Nanoengineered Morphology and Optics" *SPIE*, 2005, Bellingham, WA.

Lakowicz, J. R. (2001) "Radiative decay engineering" *Anal. Biochem*. 298, 1.

Lakowicz, J. R.; Shen Y, D'Auria, S.; Malicka J.; Fang J.; Gryczynski Z.; and Gryczynski I.; (2002) "Radiative decay engineering: Effects of Silver Island Films on Fluorescence Intensity, Lifetimes, and Resonance Energy Transfer"*Anal. Biochem*. 301, 261-277.

Lee K. S.; El-Sayed M.A.; (2005) "Dependence of the Enhanced Optical Scattering Efficiency Relative to That of Absorption for Gold Metal Nanorods on Aspect Ratio, Size, End-Cap Shape, and Medium Refractive Index" *J. Phys. Chem. B* 109, 20331.

Lee K. S.; El-Sayed M.A.; (2006) "Gold and Silver Nanoparticles in Sensing and Imaging: Sensitivity of Plasmon Response to Size, Shape, and Metal Composition" *J. Phys. Chem. B* 110, 19220.

Li P. C.; Wei C. W.; Liao C. K.; Chen C. D.; Pao K. C.; Wang C. R. C.; Wu Y. N.; and Shieh D. B.; (2006) "Multiple targeting in photoacoustic imaging using bioconjugated gold nanorods," *Photons Plus Ultrasound: Imaging and Sensing 2006: The 7th Conference on Biomedical Thermoacoustics, Optoacoustics, and Acousto-optics, Proc. of SPIE*, vol. 6086, p. 60860M.

Liang, H. Y.; Yang, H. X.; Wang, W. Z.; Li, J. Q.; Xu, H. X. (2009) "High-Yield Uniform Synthesis and Microstructure-Determination of Rice-Shaped Silver Nanocrystals" *J. Am. Chem. Soc.* 131, 6068– 6069.

Liebermann, T.; Knoll, W.; (2000) "Surface plasmon field-enhanced fluorescence spectroscopy"*Colloid Surf. A 171* (1-3), 115–130.

Link S.; Mohamed M. B.; and El-Sayed M. A.; (1999) "Simulation of the Optical Absorption Spectra of Gold Nanorods as a Function of Their aspect Ratio and the Effect of the Medium Dielectric Constant" *J. Phys. Chem. B 103,* 3073-3077.

Liu Y. J.; Fan J. G.; Zhao Y. P.; Shanmukh S.; and R. Dluhy R. A.; (2006) "Angle dependent surface enhanced Raman scattering obtained from a Ag nanorod array substrate," *Appl. Phys. Lett*, 89, 173134.

Messaier R.; Latakhia A.; (1999) "Scalptured thin films II Experiments and applications" *Mater. Res. Innovations* 2, 217.

Ming T.; Zhao L.; Yang Z.; Chen H.; Sun L.; Wang J.; and Yan C.; (2009) "Strong Polarization Dependence of Plasmon-Enhanced Fluorescence on Single Gold Nanorods", *Nano letters*, 11, 3896-3903.

Mohamed M. B.; Volkov V.; Link S.; El-Sayed M. A.; (2000) "The 'lightning' gold nanorods: fluorescence enhancement of over a million compared to the gold metal" *Chem. Phys. Lett.* 317, 517–523

Murphy C. J.; San T. K.; Gole A. M.; Orendorff C. J.; Gao J. X.; Gao J, Gou L.; Hunyadi S. E.; Li T.; (2005) "Anisotropic metal nanoparticles: synthesis, assembly, and optical applications". *J Phys Chem B* 109:13857–13870.

Nicewarner-Pena, S. R.; Freeman, R. G.; Reiss, B. D.; He, L.; Pena, D. J.; Walton, I. D.; Cromer, R.; Keating, C. D.; Natan, M. J.; (2001) "Submicrometer Metallic Barcodes" *Science*, 294, 137

Niidome T.; Yamagata M.; Okamoto Y.; Akiyama Y.; Takahashi H.; Kawano T.; Katayama Y.; Niidome Y.; (2006) "PEG-modified gold nanorods with a stealth character for *in vivo* applications" *J. Controlled Release*, 114, 343.

Nikoobakht B.; El-Sayed M. A.; (2003) "Preparation and Growth Mechanism of Gold Nanorods (NRs) Using Seed-Mediated Growth Method," *Chem. Mater.* 15, 1957.

Novo C.; Gomez D.; Perez-Juste J.; Zhang Z.; Petrova H.; Reismann M.; Mulvaney P.; Hartland G. V.; (2006) "Contributions from Radiation Damping and Surface Scattering to the Linewidth of the Longitudinal Plasmon Band of Gold Nanorods: A Single Particle" *Phys. Chem. Chem. Phys*., 8, 3540.

Obare S. O.; Jana N. R.; Murphy C. J.; (2001) "Preparation of Polystyrene and Silica-Coated Gold Nanorods and their use as Templates for the Synthesis of Hollow Nanotubes," *Nano Lett*. 1, 601.

Oyelere A. K.; Chen B.; Huang X.; El-Sayed I. H.; El-Sayed M. A.; (2007) "Peptide-Conjugated Gold Nanorods for Nuclear Targeting" *Bioconjug. Chem*., 18, 1490.

P´erez-Juste J.; Pastoriza-Santos I.; Liz-Marzan L M.; Mulvaney P.; (2005) "Gold nanorods: Synthesis, characterization and applications" *Coordination Chemistry Reviews* 249, 1870–1901.

Pietrobon, B.; McEachran M.; and Kitaev V.; (2009) "Synthesis of Size-Controlled Faceted Pentagonal Silver Nanorods with Tunable Plasmonic Properties and Self-Assembly of These Nanorods" *ACS Nano*, 3, 21–26.

G. Schider, J. Krenn R.; Hohenau A.; Ditlbacher H.; Leitner A.; Aussenegg F. R.; Schaich W. L.; Puscasu I.; Monacelli B.; and Boreman G.; (2003) "Plasmon dispersion relation of Au and Ag nanowires" *Phys. Rev. B*, *68*, 155427.

Shanmukh S. S.; Jones L.; Driskell J.; Zhao Y.; Dluhy R.; and Tripp R. A.; (2006) "Rapid and sensitive detection of respiratory virus molecular signatures using a silver nanorod array SERS substrate," *Nano Lett*. 6, 2630

Slaughter L.S.; Wu Y.P.; Willingham B.; Nordlander P.; and Link S.; (2010) "*Effects of symmetry breaking and conductive contact on the plasmon coupling in gold nanorod dimmers", ACS Nano* 4, 4657-4666.

Smythe E. J.; Cubukcu E.; Capasso F.; (2007) "Optical Properties of Surface Plasmon Resonances of Coupled Metallic Nanorods" *Opt. Express* 15, 7439.

Sokolov, K.; Chumanov, G.; Cotton, T. M. (1998) "Enhancement of Molecular Fluorescence near the Surface of Colloidal Metal Films" *Anal. Chem. 70* (18), 3898–3905.

Sonnichsen C.; Franzl T.; Wilk T.; Plessen G. V.; Feldmann J.; (2002) "Drastic Reduction of Plasmon Damping in Gold Nanorods" *Phys. Rev. Lett.* 88, 077402.

Su K. H.; Wei Q. H.; Zhang X.; Mock J. J.; Smith D. R.; Schultz S.; (2003) "Interparticle coupling effects on plasmon resonances of nanogold particles" *NanoLett.* 3, 1087.

Tao A.; Kim F.; Hess C.; Goldberger J.; He R.; Sun Y.; Xia Y.; and Yang P.; (2003) "Langmuir-Blodgett Silver Nanowire Monolayers for Molecular Sensing Using Surface-Enhanced Raman Spectroscopy", *Nano letters*, 3, 1229-1233.

Tarcha, P. J.; DeSaja-Gonzalez, J.; Rodriguez-Llorente, S.; Aroca, R. (1999) "Surface-Enhanced Fluorescence on SiO2-Coated Silver Island Films "*Appl. Spectrosc. 53* (1), 43–48.

Wiley B.; Sun Y.; Mayers, B. and Xia, Y. N. (2005). "Shape-controlled synthesis of metal nanostructures: The case of silver". *Chemistry-A European Journal,* 11, 454-463.

Wiley B.; Sun Y, and Xia, Y. (2007) "Synthesis of silver nanostructures with controlled shapes and properties". *Accounts of Chemical Research,* 40, 1067-1076.

Wiley B, Sun Y.; Chen J.; Cang H.; Li Z-Y.; Xingde L.; Xia Y. (2005) "Shape-controlled synthesis of silver and gold nanostructures". *MRS Bulletin,* 30, 356-361,

Wiley, B.; Sun, Y.; Yu YY.; Chang S-S.; Lee C-L.; Wang C. C. R.; (1997)."Gold nanorods: electrochemical synthesis and optical properties". *J Phys Chem B* 101, 6661–6664.

Xia, Y.; Xiong, Y.; Lim, B. & Skrabalak, S. E.; (2009) "Shape-controlled synthesis of metal nanocrystals: Simple chemistry meets complex physics" *Angewandte Chemie – International Edition,* 48, 60-103.

Yelin D.; Oron D.; Thiberge S.; Moses E.; Silberberg Y.; (2003) "Multiphoton Plasmon-Resonance Microscopy" *Opt. Express* 11, 1385.

Zhou Z.; Li M.; Yang Z.; Peng X.; Su X.; Zhang Z.; Li J.; Kim N.; Yu X.; Zhou L.; Hao Z.; and Wang Q.; (2010) "Plasmon-Mediated Radiative Energy Transfer across a Silver Nanowire Array *via* Resonant Transmission and Subwavelength Imaging" *ACS Nano*, 4, 5003-5010.

Nanowires - Fundamental Research

Edited by Dr. Abbass Hashim

ISBN 978-953-307-327-9
Hard cover, 552 pages
Publisher InTech
Published online 19, July, 2011
Published in print edition July, 2011

Understanding and building up the foundation of nanowire concept is a high requirement and a bridge to new technologies. Any attempt in such direction is considered as one step forward in the challenge of advanced nanotechnology. In the last few years, InTech scientific publisher has been taking the initiative of helping worldwide scientists to share and improve the methods and the nanowire technology. This book is one of InTechâ€™s attempts to contribute to the promotion of this technology.

How to reference

In order to correctly reference this scholarly work, feel free to copy and paste the following:

Goldys and Krystyna Drozdowicz-Tomsia (2011). Gold and Silver Nanowires for Fluorescence Enhancement, Nanowires - Fundamental Research, Dr. Abbass Hashim (Ed.), ISBN: 978-953-307-327-9, InTech, Available from: http://www.intechopen.com/books/nanowires-fundamental-research/gold-and-silver-nanowires-for-fluorescence-enhancement

INTECH
open science | open minds

InTech Europe
University Campus STeP Ri
Slavka Krautzeka 83/A
51000 Rijeka, Croatia
Phone: +385 (51) 770 447
Fax: +385 (51) 686 166
www.intechopen.com

InTech China
Unit 405, Office Block, Hotel Equatorial Shanghai
No.65, Yan An Road (West), Shanghai, 200040, China
中国上海市延安西路65号上海国际贵都大饭店办公楼405单元
Phone: +86-21-62489820
Fax: +86-21-62489821

IntechOpen